https://doi.org/10.1016/j.scitotenv.2015.09.093

Ambient volatile organic compounds and their effect on ozone production in Wuhan, central China

X.P. Lyu[1], N. Chen[2], H. Guo[1]*, W.H. Zhang[3]*, N. Wang[1], Y. Wang[1], M. Liu[1]

[1] Department of Civil and Environmental Engineering, The Hong Kong Polytechnic University, Hong Kong

[2] Hubei Provincial Environment Monitoring Center, Wuhan, China

[3] Department of Environmental Sciences, School of Resource and Environmental Sciences, Wuhan University, Wuhan, China

* Corresponding authors: H Guo (ceguohai@polyu.edu.hk) and WH Zhang (00007335@whu.edu.cn)

Abstract: Ambient volatile organic compounds (VOCs) were continuously measured from February 2013 to October 2014 at an urban site in Wuhan. The characteristics and sources of VOCs and their effect on ozone (O_3) formation were studied for the first time. The total VOC levels in Wuhan were relatively low, and of all VOCs, ethane (5.2 ± 0.2 ppbv) was the species with the highest levels. Six sources, *i.e.*, vehicular exhausts, coal burning, liquefied petroleum gas (LPG) usage, the petrochemical industry, solvent usage in dry cleaning/degreasing, and solvent usage in coating/paints were identified, and their contributions to the total VOCs were 27.8 ± 0.9%, 21.8 ± 0.8%, 19.8 ± 0.9%, 14.4 ± 0.9%, 8.5 ± 0.5%, and 7.7 ± 0.4%, respectively. Model simulation of a photochemical box model incorporating the Master Chemical Mechanism (PBM-MCM) indicated that the contribution to O_3 formation of the above sources was 23.4 ± 1.3%, 22.2 ± 1.2%, 23.1 ± 1.7%, 11.8 ± 0.9%, 5.2 ± 0.4%, and 14.2 ± 1.1%, respectively. LPG and solvent usage in coating/paints were the sources that showed higher contributions to O_3 formation, compared to their contributions to VOCs. The relative incremental reactivity (RIR) analysis revealed that the O_3 formation in Wuhan was generally VOC-limited, and ethene and toluene were the primary species contributing to O_3 production, accounting for 34.3% and 31.5% of the total RIR-weighted concentration, respectively. In addition, the contribution of CO to the

O_3 formation was remarkable. The C_4 alkanes and alkenes from the LPG usage also significantly contributed to the O_3 formation. The results can assist local governments in formulating and implementing control strategies for photochemical pollution.

Keywords: VOCs; source contribution; O_3 formation; RIR; PBM-MCM

1. Introduction

Ambient VOCs are important in the formation of O_3 and secondary organic aerosols (SOAs) (Guo et al., 2013; Cheng et al., 2010; Camredon et al., 2007; Tsigaridis et al., 2005). As key O_3 precursors, VOCs react with nitrogen oxides (NO_x) in the presence of sunlight, leading to photochemical pollution with elevated O_3 concentration. Due to intense and uncontrolled emissions of VOCs, mega-cities and city clusters in China, such as Beijing (Yao et al., 2015; Wei et al., 2014), the Yangtze River Delta of eastern China (Li et al., 2014; Xue et al., 2014), and the Pearl River Delta (PRD) of southern China (Ling et al., 2011; Cheng, et al., 2010) currently suffer from severe photochemical pollution.

Identifying the sources of VOCs is crucial for local government to formulate and implement emission reduction strategies, but the sources depend largely on energy consumption levels and the industrial structures of a city/region, and are often complex. In general, VOCs sources include emissions from gasoline-, diesel-, and liquefied petroleum gas (LPG)-fuelled vehicles, fuel evaporation, emissions from industries such as shoe making, furniture manufacturing and etc., solvents in paints and consumer products, and coal and biomass burning (Guo et al., 2004, 2011; Li et al., 2014; Wang et al., 2013; Cai et al., 2010). The source contributions to ambient VOCs vary between cities and regions. For example, Wang et al. (2013) found that coal burning contributed 26-39% and vehicular exhausts 31-45% to the total VOCs in Beijing in winter, while An et al. (2014) indicated that industrial emissions constituted a considerable proportion (45-63%) of the total VOCs in the Yangtze River Delta, and Cai et al. (2010) reported that industry accounted for 36% of the ambient VOCs in Shanghai. Guo et al. (2011) and Ling et al. (2011) found that solvent usage was the major source of ambient VOCs in the PRD region, whereas vehicular emissions made the most significant contribution in Hong Kong, although it is adjacent to the PRD region (Ou et al., 2015).

VOCs contribute to O_3 formation through a series of photochemical reactions, including the hydroxyl radical (OH) initiated oxidation of VOCs, nitrogen cycling driven by peroxyl (RO_2) and hydroperoxyl (HO_2) oxidation and photolysis, and the combination of oxygen atoms (O) with molecular oxygen (O_2) (Ling et al., 2014; Cheng et al., 2013). The photochemical reactivity of the VOC species and the intermediates therefore significantly influences O_3 production, along with the level of concentration. For instance, alkenes and aromatics are highly reactive in photochemical O_3 formation (Ling and Guo, 2014; Ling et al., 2011). The relative incremental reactivity (RIR) method proposed by Carter and Atkinson (1989) is frequently used to evaluate the sensitivity of O_3 production to the change of VOC precursors, through the application of an observation-based model (OBM) using the carbon bond IV mechanism. Ling et al. (2011) recently developed a combined application of the positive matrix factorization (PMF) model and the OBM to study the VOC source contributions to the formation of photochemical O_3 in Guangzhou and Hong Kong. Moreover, the maximum incremental reactivity (MIR), O_3 formation potential (OFP), and photochemical O_3 creation potential (POCP) have also been used to describe the contribution of VOC species to O_3 production (Barletta et al., 2002; Jenkin et al., 1999).

Wuhan is the largest megacity in central China and an important transport hub, and has experienced rapid development through growth in real estate and new technology industries such as optoelectronics, biological science, environmental science, etc. Accompanying this urbanization and industrialization is air pollution, characterized by haze and photochemical smog, which has been often observed in recent years. Even so, there are virtually no published studies on ambient VOCs in Wuhan. Obtaining first-hand information on VOC characteristics and sources and their association with photochemical smog formation is therefore an urgent task. To our best knowledge, this is the first study on VOC sources and their effects on the O_3 formation in this region.

In this study, the characteristics of ambient VOCs and their effects on O_3 production in Wuhan were investigated. The abundance and temporal patterns of VOCs are discussed, and the source contributions to ambient VOCs quantified. The dominant factors affecting the photochemical O_3 formation were determined using a photochemical box model incorporating the Master Chemical Mechanism (PBM-MCM), and the contributions of VOC sources to the O_3 formation were also

quantified. The O_3-precursor relationships were also evaluated using RIR and RIR-weighted concentration. The outcomes will be of help to air scientists and local governments, for further study and to take measures to reduce VOC and O_3.

2. Methodology

2.1 Site description and chemical analysis

From February 2013 to October 2014, 99 VOCs consisting of 56 non-methane hydrocarbons, 28 halocarbons, and 15 oxygenated VOCs (OVOCs), the five trace gases SO_2, NO_2, NO, CO, and O_3, and two meteorological parameters (temperature and humidity) were simultaneously monitored at an urban site (30.54 N, 114.37 E, <50 m a.s.l.) in Wuhan. The site was set up on the rooftop of a six-storey building (~18 m height) within the Hubei Provincial Environmental Monitoring Center, as shown in Figure 1.

Figure 1 Geographic location of the sampling site. The yellow blocks, crisscrossed lines, and the red spot represent the urban area, the transport network, and the sampling site, respectively

Ambient air was continuously drawn through a PFA Teflon tube with an inside diameter of 7.6 cm. The sampling tube inlet was 1.5 m above the rooftop, and the outlet was connected to a PFA-made manifold with a bypass pump drawing air at a rate of 15 L/min. A chromatography-

flame ionization detector-mass spectrometry (GC-FID-MS) system (TH_PKU-300), developed by Tianhong instrument Inc. in Wuhan and Peking University, was used to carry out real-time measurements of VOCs. The air samples were pre-concentrated by passing them through a cold trap maintaining -80 ℃ for the removal of water and carbon dioxide, and then trapped at -150 ℃ with an empty capillary column. After pre-concentration, the VOCs were desorbed by rapid heating up to 100 ℃ and introduced into the GC-FID-MS system (Agilent GC7820/5975MS) for chemical analysis. The detection limit range was 0.005 - 0.050, 0.002 - 0.021, 0.002 - 0.023, and 0.011 - 0.070 ppbv for C_2 - C_5 hydrocarbons, C_6 – C_9 hydrocarbons, halocarbons, and OVOCs with R^2 ≥0.996, ≥0.993, ≥0.998, and ≥0.985, respectively (more details can be found in the supplementary material - Table S1).

Commercial instruments developed by Thermo Environmental Instruments (TEI) Inc. were used to measure the trace gases. SO_2, NO_x (NO_x = NO + NO_2), CO, and O_3 were detected with a pulsed UV fluorescence SO_2 analyzer (Model 43, TEI), a chemiluminescence trace level NO-NO_2-NO_x analyzer (Model 42*i*TL, TEI), an enhanced trace level CO analyzer (Model 48*i*TL, TEI), and an UV photometric O_3 analyzer (Model 49*i*, TEI), respectively. Details of the instruments including the operating principles, measuring ranges, and detection limits were provided by Geng et al. (2009) and Chang et al. (2007).

2.2 Quality assurance and control (QA/QC)

To guarantee the data quality acquired from the TH_PKU-300 system, the calibration of sampling flow rate, mass spectrometer tuning, blank experiment, and instrument calibration were conducted regularly. The sampling flow rate was calibrated every six months with an electronic soap film flow meter (Sensidyne, Gilibrator-2) to ensure the sampling flow precision was in the range of ± 1.5%. The mass spectrometry was tuned before the MS analysis, to make sure that the half peak width (PW_{50}) was between 0.45 - 0.55 on the contour map, and the peak shape was symmetric with no bifurcation. The concentrations of VOC species in the blank experiments were all below 5% of the average concentrations of VOCs in ambient air. The GC-FID-MS system was calibrated every two weeks with six concentration levels of standard samples in the range of 0.3 - 25 ppbv, and the standard sample with the same concentration level was analyzed three times. A standard sample with moderate concentration (*i.e.*, the concentration near the

middle of the calibration curve) was applied to test the performance of the system at 00:00 every day, the acceptable standard deviation (SD) was ≤20%, and therefore the data of VOCs at 00:00 were excluded from the study. The duplicate tests (7-10 times) of the VOCs with the lowest concentration at the standard curve indicated that the SD was lower than 10%.

2.3 Model description

2.3.1 PMF receptor model

Based on the chemical mass balance between measured species concentrations and source profiles, PMF treats the measured *j* species concentration in *i* sample (x_{ij}) as the sum of contributions from *p* sources, which can be divided into contribution *G* and source profile *F*, as shown in equation (1) (Paatero, 1997; Paatero and Tapper, 1994):

$$x_{ij} = \sum_{k=1}^{p} g_{ik} f_{kj} + e_{ij} \qquad (1)$$

where g_{ik} is the species contribution of the *k*th source to the *i*th sample, f_{kj} is the species fraction in *k*th source, and e_{ij} is the residual associated with species *j* in sample *i*. Details about the PMF operation is provided in Guo et al. (2011).

The matrices of G and F are obtained in the case of the minimum of objective function Q, as shown in equation (2):

$$Q = \sum_{i=1}^{n} \sum_{j=1}^{m} \left[\frac{x_{ij} - \sum_{k=1}^{p} g_{ik} f_{kj}}{u_{ij}} \right]^2 \qquad (2)$$

where *m* and *n* represent the number of species and samples, respectively, and u_{ij} is the uncertainty of *j* species in the *i* sample. Q (robust) is automatically calculated by excluding the points not fit by the model, and the run with the lowest Q (robust) value is selected as the optimum solution by the model.

2.3.2 PBM-MCM model

The PBM-MCM model is a zero dimension photochemical box model combined with a near explicit chemical mechanism consisting of 5,900 species and 16,500 reactions, which fully describe the mechanisms of homogeneous reactions in the atmosphere. The atmospheric physical

process, *i.e.*, vertical and horizontal transport is not considered in the PBM-MCM model. Details of the model construction can be found in Lam et al. (2013) and Saunders et al. (2003). Briefly, the observed data including VOCs, trace gases, and meteorological parameters were used to construct the model. Based on the observations and the chemical mechanisms integrated in the model, the photochemical production and destruction of the chemical compounds and intermediates were determined by the model simulation. The PBM-MCM model has been successfully applied in previous studies (Ling et al., 2014; Lam et al., 2013; Cheng et al., 2010). In this study, 37 VOCs, made up of 32 hydrocarbons and 5 halocarbons, five trace gases, and two meteorological parameters from the field measurements were used for model input. VOC concentrations at 0:00 were excluded, so were replaced by half of the detection limit value for each VOC species to initiate the model.

PBM-MCM with a more explicit photochemical mechanism than carbon bond IV was incorporated with PMF to evaluate the O_3 production by VOC groups/sectors and species, in addition to the simulation of O_3 production. The parameters, *i.e.*, RIR, average RIR, and RIR-weighted concentration were calculated using equations (3) - (5) (Carter and Atkinson, 1989):

$$RIR^{S}(X) = \frac{[P^{N}{}_{O_3-NO}(X) - P^{N}{}_{O_3-NO}(X-\Delta X)]/P^{N}{}_{O_3-NO}(X)}{\Delta S(X)/S(X)} \quad (3)$$

$$\overline{RIR} = \frac{\sum_1^m RIR^{N}(X) \cdot P^{N}{}_{O_3-NO}(X)}{\sum_1^m P^{N}{}_{O_3-NO}(X)} \quad (4)$$

$$\text{RIR} - \text{weighted concentration} = RIR(X) \times \text{concentration} \quad (5)$$

where $P^{N}{}_{O_3-NO}(X)$ and $P^{N}{}_{O_3-NO}(X-\Delta X)$ represent the O_3 production in a base run with original concentrations, and in a run with a hypothetical change (ΔX) (10% in this study) in source/ species X. In both runs, net O_3 production with titration by NO is considered; $S(X)$ is the measured concentration of X and $\Delta S(X)$ is the concentration change of X caused by the hypothetical change; m means the number of days simulated; and the "concentration" in equation (4) was obtained from the measurements or PMF resolutions.

3. Results and discussion

3.1 General characteristics

3.1.1 Meteorological conditions

Table 1 shows the statistics of meteorological parameters simultaneously monitored with VOCs and trace gases. The prevailing wind was from the southwest, while the wind speed was very low (1.1 ± 0.02 m/s), implying the dominance of local air masses at the monitoring site. Obvious seasonal patterns were observed, with the maximums of wind speed, temperature, and relative humidity in summer and minimums in winter. Conversely, the sea level pressure was lowest in summer and highest in winter. The seasonal variations of meteorological conditions may influence the dispersion, photochemical reactions, and emissions of air pollutants. A detailed discussion is given below.

Table 1 Statistics of meteorological parameters at the monitoring site

	Wind speed/ m/s	Wind direction/ °	Temperature/ °C	Sea level pressure/ hPa	Relative humidity/ %
Spring	1.2 ± 0.04	150.3 ± 3.4	19.0 ± 0.2	1008.3 ± 0.3	72.6 ± 0.8
Summer	1.2 ± 0.04	137.3 ± 3.3	28.4 ± 0.2	997.9 ± 0.1	82.5 ± 0.6
Autumn	1.0 ± 0.1	132.4 ± 4.3	19.0 ± 0.3	1013.2 ± 0.2	72.1 ± 0.9
Winter	0.9 ± 0.1	129.2 ± 4.8	8.0 ± 0.2	1019.4 ± 0.3	68.4 ± 1.2
Mean	1.1 ± 0.02	139.0 ± 1.9	19.4 ± 0.2	1008.8 ± 0.2	74.3 ± 0.4

3.1.2 Concentration and composition of VOCs in Wuhan

Table 2 shows the mixing ratios of total VOCs (TVOCs) and major VOC species at urban sites in Wuhan and other cities/regions in China. When available, the 95% confidence intervals are also provided here. TVOCs in Wuhan (23.3 ± 0.5 ppbv) were found to be on the low side, compared to those in Beijing (43.4 ppbv), Shanghai (32.4 ppbv), and Guangzhou (70.0 ppbv), but higher than those in Hong Kong (18.5 ± 2.1 ppbv). Ethane (5.2 ± 0.2 ppbv), ethene (3.3 ± 0.2 ppbv), and toluene (2.0 ± 0.1 ppbv) were the most abundant species in Wuhan, accounting for 40.7 ± 0.3% of the TVOCs. Generally, C_2 species are closely related to vehicular exhausts and coal/biomass burning, while solvents and vehicular exhausts are the major sources of toluene (Liu et al., 2008a; Guo et al., 2007). The abundance of C_2 species and toluene implies that the

potential VOC sources in Wuhan are vehicular exhausts and solvent usage. Compared with Beijing, Shanghai, and Guangzhou, Wuhan had a higher or at least a comparable level of ethane, though the level of TVOCs was much lower. This may be attributable to the use of natural gas (NG) as taxi fuel in Wuhan, as ethane is a major component of NG. Compared to Hong Kong, higher or comparable levels were observed for most VOCs except the solvent-related species (*i.e.* toluene and xylenes), which were significantly (p <0.05) lower in Wuhan, indicating that solvent usage has less of an effect on VOCs in Wuhan. The sampling period, sampling location, measured species, and meteorological conditions should, however, be taken into account, as these influence the concentration and composition of ambient VOCs.

3.1.3 Seasonal and diurnal patterns of VOCs

Figure 2 shows the monthly average mixing ratios of ethane, ethene, toluene, and isoprene. Though differences exist, the selected species broadly represent the respective alkanes, alkenes, aromatics, and biogenic VOCs (mainly isoprene) and their seasonal variations. The highest values of ethane, ethene, and toluene were observed in winter and the lowest in summer. The higher levels of VOCs in winter resulted from inhibited photo-degradation at low temperatures and suppressed dispersion, due to low wind speed and high pressure. Additional emissions (*i.e.* coal burning) may also be present, in view of the marked increase of 1,2-dichloroethane from 0.3 ± 0.02 ppbv in summer to 0.9 ± 0.1 ppbv in winter. Conversely, the high temperature, wind speed, and low pressure accelerate the photochemical depletion and dispersion of VOCs in summer. The wind speed at the monitoring station was low (*i.e.* 1.1 ± 0.02 m/s), so the origins of air masses could not be interpreted from the wind direction. However, previous research (Lyu et al., 2015) found that in winter local air masses and those originating from northeastern and northwestern China were dominant in Wuhan (78%), while in summer over 80% of air masses were from southern China, and over a third originated from the South and East China Seas. This may also explain the seasonal patterns of VOCs, as the continental air mass from northern China in winter was often pollutant-laden (Wang et al., 2013; Chan and Yao, 2008), while the summer marine flows should be much cleaner.

Unlike anthropogenic VOCs, isoprene levels were highest in summer and lowest in winter. Considering the conditions discussed above and the faster oxidation of isoprene by OH (Atkison, 1990), the isoprene seasonal variation suggests that biogenic emission is influenced (*i.e.*

enhanced in summer and inhibited in winter) to a greater extent by seasonal change than photochemical consumption and dispersion. This is reasonable in view of the linearly incremental leakage of isoprene below 40 °C (Sharkey et al., 1996). The higher summer level in 2013, when the temperature was significantly higher (p <0.001) than in 2014, also confirmed this assumption.

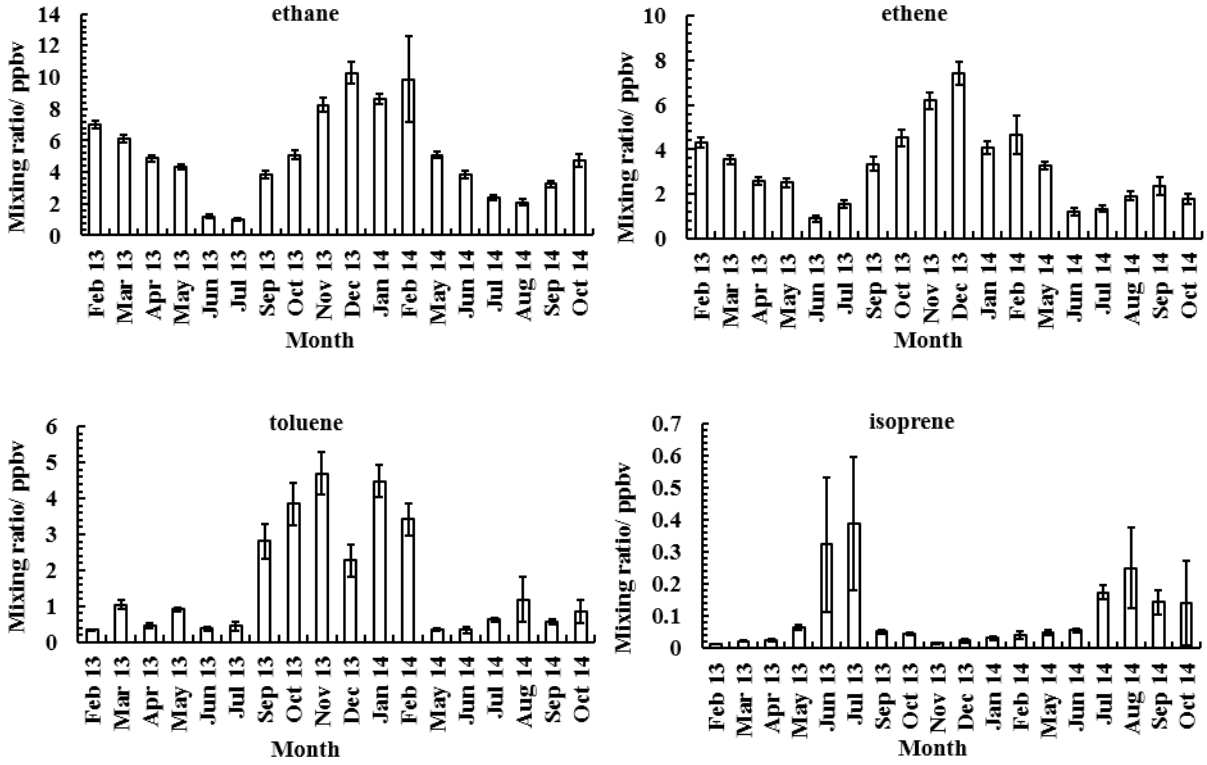

Figure 2 Seasonal patterns of ethane, ethene, toluene, and isoprene from February 2013 to October 2014. The missed months are due to instrument maintenance.

Diurnal variations of VOCs are affected by chemical and physical processes. Figure 3 shows the hourly averages of ethane, ethene, toluene, and isoprene. The nocturnal mixing ratios of ethane, ethene, and toluene were higher than those recorded in the daytime. Differences were found, but the overall diurnal trends were the same; the mixing ratios increased and reached a small peak in the morning, then decreased to their minimums in the afternoon, and returned to steadily high levels at night. The morning increase was likely due to the vehicular exhausts during peak traffic hours. The increment of ethane was very minor compared to those of ethene and toluene, which, as its possible source is NG-fueled taxis, may be related to the stable daily taxi flow. The decrease of ethane, ethene, and toluene in late morning clearly implied photo-degradation and

dispersion due to the extension of the boundary layer. From late afternoon to evening the photochemical reactions weakened, and the mixing height decreased and vehicular emissions increased in the afternoon rush hours, causing a rebound of anthropogenic VOCs.

Conversely, higher levels of isoprene were present in daytime hours than that at night, though its oxidation by OH is faster during the day (Atkison, 1990), suggesting that biogenic emission of isoprene was more enhanced than its photochemical oxidation and dispersion in the day. The high sensitivity of isoprene leakage to light and temperature is the most likely cause of this (Sharkey et al., 1996).

3.1.4 VOC ratios and O_3 formation

Ratios of VOCs with different photochemical reactivity indicate the atmospheric transport and aging process. For the ratios of a more reactive to a less reactive VOC, higher values imply fresh or local emissions, while lower values are associated with aged or long-range transported air masses (Guo et al., 2007). In this study, ratios of ethene/ethane (with lifetimes of 1.4d for ethene and 56d for ethane) (Warneck, 2000) and *m, p*-xylene/ethylbenzene (lifetimes of 0.6-1d for *m, p*-xylene and 2d for ethylbenzene) (Warneck, 2000) were calculated. Figure 4 presents the diurnal shifts of VOC ratios and O_3 mixing ratios. The mean ratios of ethene/ethane and *m, p*-xylene/ethylbenzene were 0.65±0.06 and 1.33±0.09 ppbv/ppbv, respectively, lower than those observed at an urban site in Hong Kong (0.7 ppbv/ppbv for ethene/ethane and 1.8 ppbv/ppbv for *m, p*-xylene/ethylbenzene) where photochemical pollution was predominately due to local emissions (Guo et al., 2007). VOC ratios are strongly dependent upon the local emission profiles, the sampling period, and the sampling site. Bearing these factors in mind, the lower ratios may suggest the regional/superregional transport of pollutant-laden air masses into Wuhan. From the diurnal variation, higher and more stable ratios were observed during nighttime. Both the ratios increased slightly in the morning, decreasing steadily from 09:00, were lowest in the afternoon, and returned to high values at night. The increment in the morning may be related to newly emitted VOCs from vehicles during rush hours, the decrease from morning to afternoon clearly indicated the aging process of air masses, and the rebound from afternoon to night was mainly due to weak photochemical reactions and the superimposition of fresh vehicular exhaust emissions.

The diurnal trend of O_3 was the opposite of the VOC ratios. It increased during the photochemical aging process (late morning/early afternoon), reaching a maximum in the afternoon, and then decreased to a low level at night due to fresh emissions and weak photochemical reactions. Corresponding to the morning increase of VOC ratios, a slight trough of O_3 was observed, mainly due to the enhanced titration by NO, which increased by 85% from 13.6±4.0 ppbv at 06:00 to 25.2±4.8 ppbv at 08:00. It is evident that O_3 variation in Wuhan was closely associated with photochemical reactions.

Table 2 Comparisons of TVOCs and major VOC species measured in Wuhan and other cities/regions in China

Species	Wuhan (this study) (2013-2014)		Beijing [a] (August, 2005)	Shanghai [b] (2007-2010)	Guangzhou [c] (October-November, 2004)	Hong Kong [d] (2002-2003)		43 Chinese cities [e] (January-February, 2001)	
	Mean	95% confidence interval	Mean	Mean	Mean	Mean	95% confidence interval	Min	Max
ethane	5.2	0.2	3.8	-	5.6	1.8	0.3	3.7	17.0
ethene	3.3	0.2	4.6	-	6.6	1.5	0.2	2.1	34.8
ethyne	1.9	0.1	5.4	-	7.3	2.0	0.3	2.9	58.3
propane	1.9	0.1	3.6	4.8	10.4	1.6	0.2	1.5	20.8
propene	0.5	0.01	1.2	0.8	3.0	0.3	0.04	0.2	8.2
i-butane	1.1	0.03	2.3	1.4	2.9	0.9	0.1	0.4	4.6
n-butane	1.3	0.1	2.8	2.0	5.1	1.5	0.2	0.6	14.5
1-butene	0.3	0.02	1.0	0.3	1.3	0.1	0.01	0.07	2.4
1,3-butadiene	0.2	0.01	-	-	0.2	0.1	0.01	0.02	2.5
i-pentane	1.0	0.03	4.1	2.3	2.6	0.5	0.1	0.3	18.8
n-pentane	0.5	0.02	1.7	-	1.2	0.3	0.03	0.2	7.7
n-hexane	0.1	0.01	0.7	0.8	0.8	-	-	0.1	3.2
n-heptane	0.1	0.02	-	0.2	0.6	-	-	0.06	3.4
n-octane	0.1	0.01	-	-	0.2	-	-	0.04	1.3
benzene	1.7	0.01	1.8	1.8	2.4	0.4	0.1	0.7	10.4
toluene	2.0	0.1	3.0	4.7	7.0	2.8	0.4	0.4	11.2
ethylbenzene	0.5	0.01	1.0	1.2	1.2	0.4	0.1	0.1	2.7
m, p-xylene	0.4	0.01	2.0	1.4	1.5	0.7	0.1	0.4	15.3
o-xylene	0.2	0.01	0.9	0.5	0.5	0.2	0.03	0.1	6.9
TVOCs	24.3	0.5	43.4	32.4	70.0	18.5	2.1	-	-

Units are in ppbv unless otherwise specified.

[a] Song et al. (2007); [b] Cai et al. (2010); [c] Liu et al. (2008); [d] Guo et al. (2007); [e] Barletta et al. (2005)

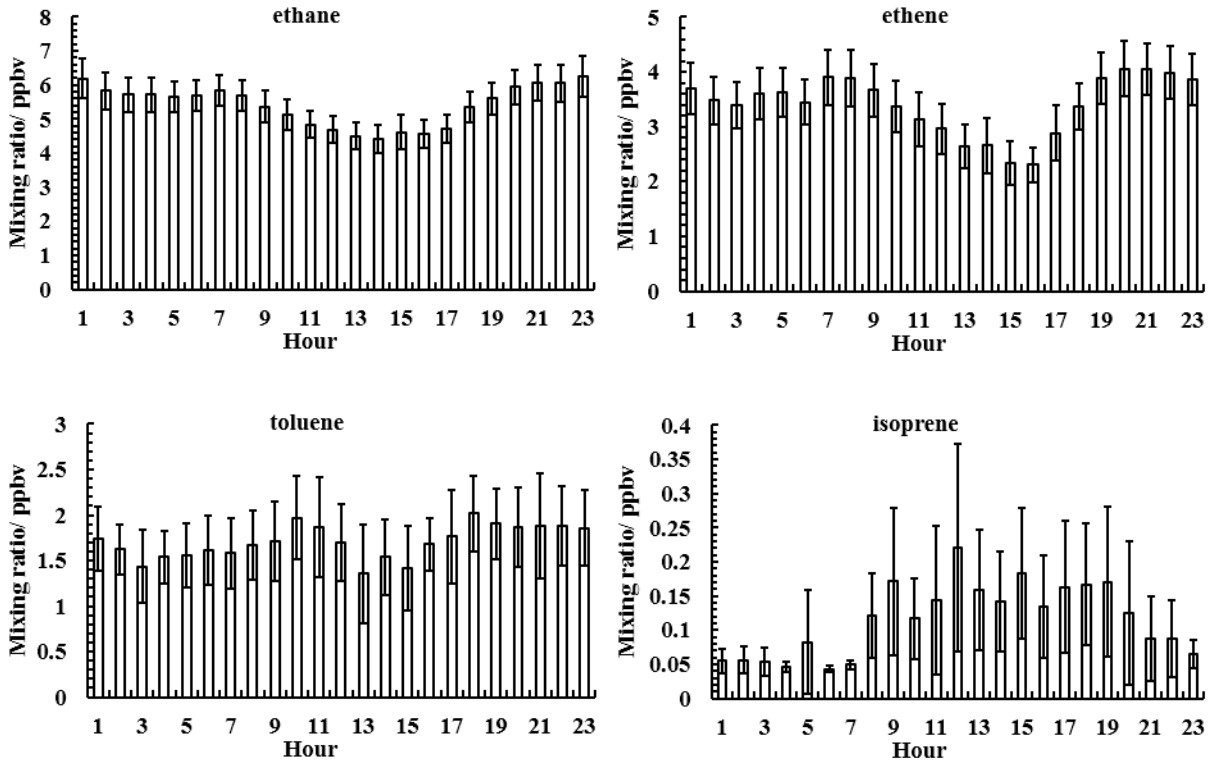

Figure 3 Hourly averages of ethane, ethene, toluene, and isoprene from February 2013 to October 2014. The values at 00:00 were excluded due to daily calibration.

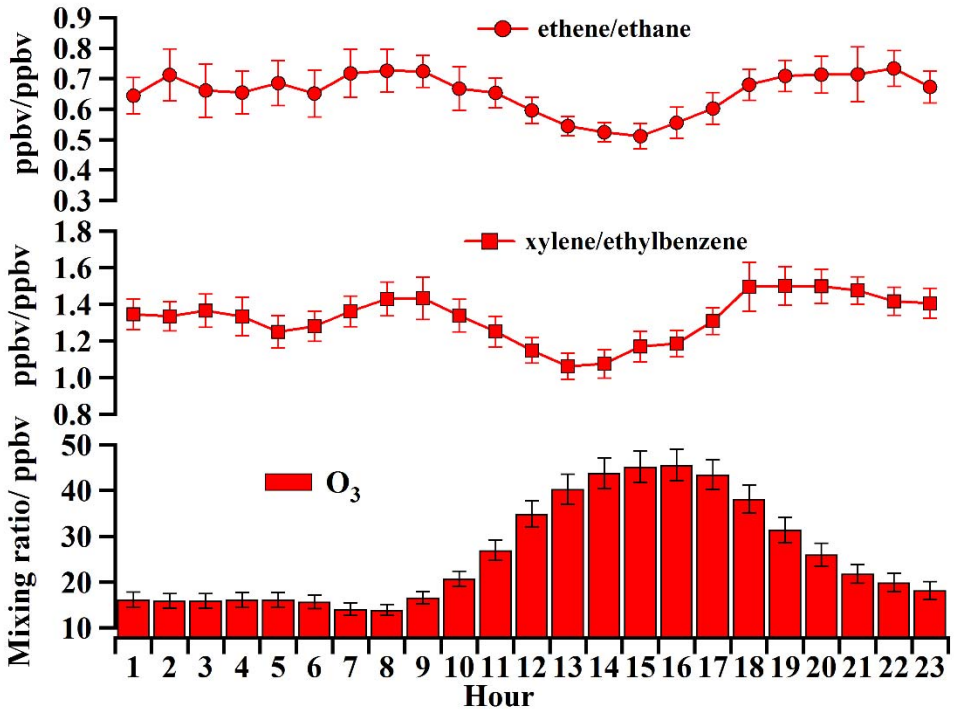

Figure 4 Diurnal variations of ethene/ethane, xylene/ethylbenzene, and O_3 mixing ratio from February 2013 to October 2014. The values at 00:00 were excluded due to daily calibration.

3.2 Sources of VOCs

3.2.1 Source identification

Based on the principle that each factor can be exclusively indicated by the tracers of one source, a six-factor resolution with the lowest Q value was obtained to best reproduce the measured concentrations of VOCs. Figure 5 shows the source profiles of the six resolved factors. The first had high loadings of C_2 – C_3 hydrocarbons, *n/i*-pentanes, and moderate percentages of SO_2, NO_2, and CO. These species are all closely related to the exhausts of internal-combustion engines (Liu et al., 2008a; Guo et al., 2004). Factor 1 is therefore assigned to vehicular exhausts. The second factor was distinguished by a high percentage of 1, 2-dichloroethane, BTEX, and SO_2. This is usually associated with coal burning (Cai et al., 2010; Liu et al., 2008a). Factor 3, dominated by *trans*-2-butene, 1-butene, and *n/i*-butanes, was likely derived from LPG usage (Song et al., 2008; Guo et al., 2004, 2007). It is noteworthy that there are no LPG-fueled vehicles in Wuhan, but catering and household LPG use is widespread. This factor is therefore identified as LPG usage in households and catering. The fourth factor contained most of the vinyl chloride, 1, 3-butadiene, and some C_2-C_4 hydrocarbons, which have been identified in the emissions of the petrochemical industry (Cetin et al., 2003; Na et al., 2001). 1, 3-butadiene is also an important pyrolysis product of crude oil and gas (Morrow, 1990). Therefore, factor 4 is assigned to the petrochemical industry. Factor 5 appeared to be associated with solvent usage, with high loadings of C_6 - C_7 alkanes and moderate percentages of trichloroethylene and tetrachloroethylene, which serve as solvents in dry cleaning/degreasing (An et al., 2014; Huang et al., 2014; Kwon and Lee, 2003; Lash and Parker, 2001). The last factor had high loadings of nonane and decane, and moderate percentages of TEX (toluene/ethylbenzene/xylenes). This factor is identified as solvent usage in painting/coating, as high levels of nonane and decane can be emitted from asphalt application (*i.e.* coating) (Liu et al., 2008a; Brown et al., 2007), and TEX often represents solvent emissions (*i.e.* paints) (Ou et al., 2015).

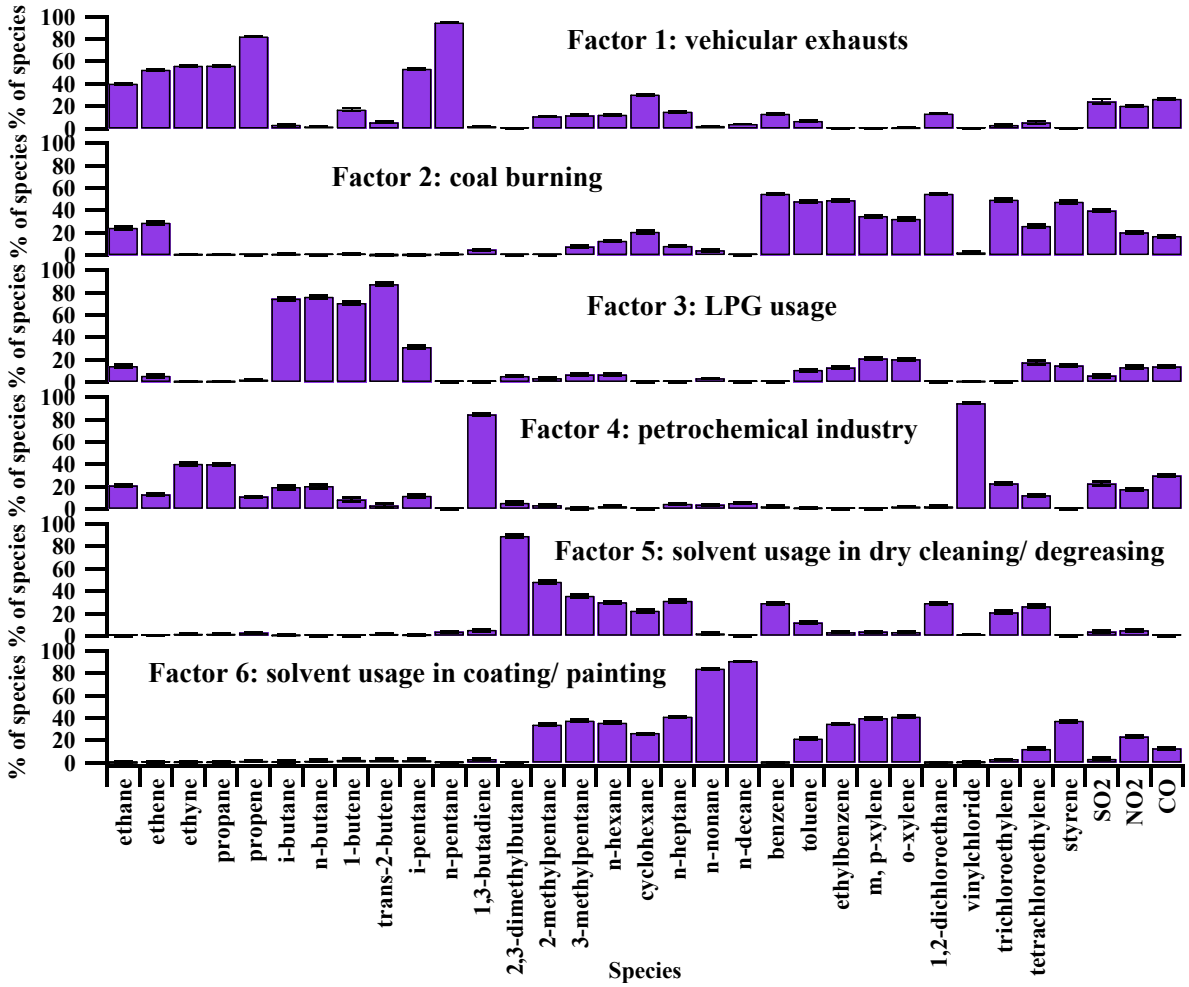

Figure 5 PMF-extracted source profiles of VOCs in Wuhan. The error bars were estimated using the bootstrap method integrated in PMF.

3.2.2 Source apportionment

Table 3 presents the concentration and percentage contribution of the identified sources. Vehicular exhausts (27.8 ± 0.9%) and coal burning (21.8 ± 0.8%) were the main contributors to VOCs in Wuhan. Of the compared Chinese cities/regions, the contribution of vehicular exhausts to VOCs in Wuhan was lower than that in PRD (>50%) (Liu et al., 2008b) and Beijing (57.7%) (Liu et al., 2005), and comparable to Shanghai (25%) (Cai et al., 2010). However, the contribution of coal burning was much higher in Wuhan than in southern and eastern China (<10%) (Huang et al., 2011; Cai et al., 2010; Liu et al., 2008b). The contribution of LPG (19.8 ± 0.9%) was much lower than in Hong Kong (32.6 ± 5.8%) (Ou et al., 2015), and comparable to or even higher than in PRD (8% - 16%) (Liu et al., 2008b). Given that there are no LPG-fueled

vehicles in Wuhan, the emissions of LPG-related VOCs from household and catering was considerable. The contribution of the petrochemical industry to VOCs is seldom quantified in China, but this cannot be neglected in Wuhan, the location of the largest refinery base in central China. The contribution of solvent usage in dry cleaning/degreasing and painting/coating (16.2 ± 0.9%) was comparable to that in PRD (19.5 ± 8.5%) (Liu et al., 2008b), but much less than that in Hong Kong (58.0 ± 12.1%) (Ou et al., 2015). Nevertheless, source identification and source contributions strongly depend upon the species and profiles used for source apportionment, and the study period.

Table 3 Source contributions to the measured VOCs in Wuhan (mean±95%C.I.)

	Concentration (μg/m^3)	Contribution (%)
Vehicular exhausts	13.9±0.5	27.8±0.9
Coal burning	10.9±0.4	21.8±0.8
LPG usage	9.9±0.5	19.8±0.9
Petrochemical industry	7.2±0.5	14.4±0.9
Dry cleaning/degreasing	4.3±0.3	8.5±0.5
Painting/ coating	3.8±0.2	7.7±0.4

3.3 O_3 production by VOC sources

Before studying the effect of VOCs on O_3 production, the PBM-MCM model was validated. Figure 6 compares monthly average diurnal (07:00 – 19:00) variations of simulated and observed O_3. It is noticeable that the model simulated the diurnal trends of O_3 well, which began to increase in the morning, reaching maximums in the afternoon, and decreasing to low levels at night. The simulated maximums and minimums coincided with the observations in the range of ±30%, except for the months of February, July, September, and October 2013, when the simulated O_3 was much higher (~80%). Indeed, the simulated values were generally higher than the observations. This discrepancy is probably because the PBM-MCM model does not consider the processes of horizontal and vertical transport, which actually affect the concentration of air pollutants. To quantitatively evaluate the performance of the model, the index of agreement (IOA) was calculated as follows (Huang et al., 2005):

$$IOA = 1 - \frac{\sum_{i=1}^{n}(O_i - S_i)^2}{\sum_{i=1}^{n}(|O_i - \bar{O}| + |S_i - \bar{O}|)^2}$$

where O_i, S_i, and $\bar{O}$ represent the hourly observation, the simulation, and the average of observations, respectively. In the range of [0 - 1], a higher IOA indicates better agreement between simulated and observed values. The IOA was calculated as 0.74, indicating the acceptable performance of the PBM-MCM model in simulating O_3 formation in Wuhan.

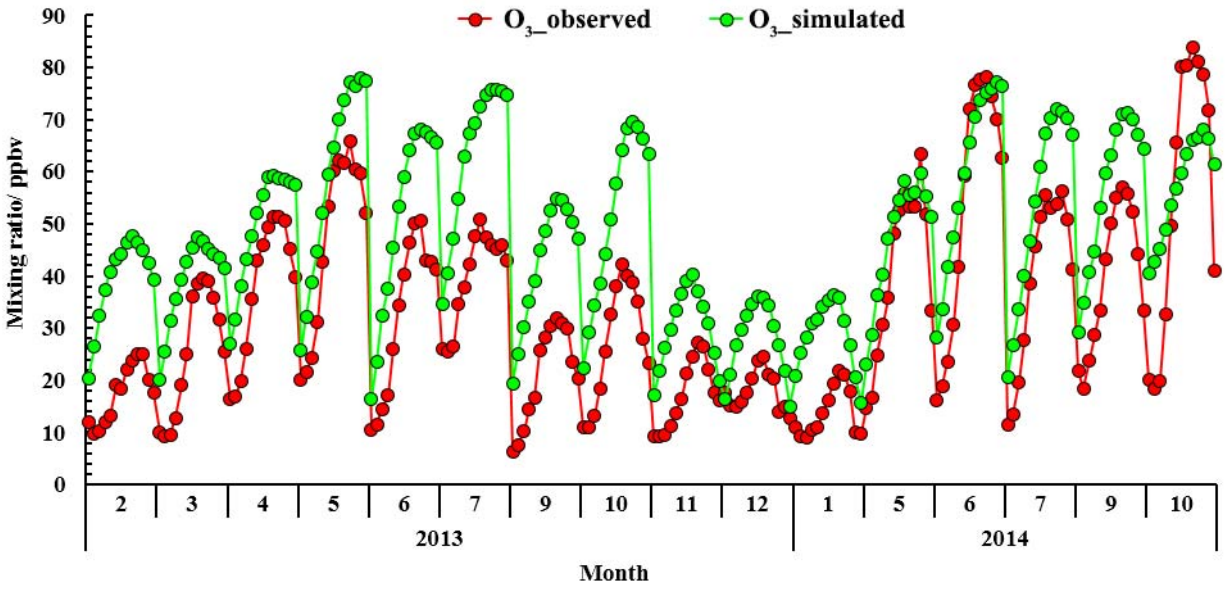

Figure 6 Comparison between the simulated and observed O_3 from 07:00 to 19:00. The missed months were due to instrument maintenance.

Two scenarios of simulation, the original using the observed data and the constrained scenario using the data with VOCs in source *i* cut, were conducted to study the effect of VOC source *i* on O_3 production. The difference between these two scenarios was the net simulated O_3 production by source *i*. It should be noted that this value represents the photochemical O_3 formation without considering the background O_3, or the O_3 transported from the free troposphere. Table 4 summarizes the contribution of each source to O_3 production and to VOC concentration. LPG usage (23.1±1.7%) and solvent usage in painting and coating (14.2±1.1%) were found to make a much higher contribution (p<0.05) to O_3 production compared to their contributions to VOCs (19.8±0.9% and 7.7±0.4, respectively). In contrast, the contributions to O_3 production by vehicular exhausts (23.4±1.3%), the petrochemical industry (11.8±0.9%), and solvent usage in

dry cleaning and degreasing (5.2±0.4%) were relatively lower than their contributions to VOCs (27.8±0.9%, 14.4±0.9%, and 8.5±0.5%, respectively). These results suggest that the contribution of a source to VOCs is often different from its contribution to O_3 production, highlighting the importance of the photochemical reactivity of VOCs.

Table 4 Source contributions to VOCs and O_3 production

	Contribution to VOCs (%)	Contribution to O_3 formation (%)
Vehicular exhausts	27.8 ± 0.9	23.4 ± 1.3
Coal burning	21.8 ± 0.8	22.2 ± 1.2
LPG usage	19.8 ± 0.9	23.1 ± 1.7
Petrochemical industry	14.4 ± 0.9	11.8 ± 0.9
Dry cleaning/ degreasing	8.5 ± 0.5	5.2 ± 0.4
Painting/ coating	7.7 ± 0.4	14.2 ± 1.1

3.4 O_3 - precursor relationship

3.4.1 Average RIR of VOC groups and species

RIR is a common parameter describing the reactivity of O_3 precursors. Figure 7 shows the average RIR values of anthropogenic VOCs (AHC), natural VOCs (NHC), CO, and NO. It was found that the RIR of VOCs (*i.e.* AHC and NHC) were positive. Cutting VOCs can reduce O_3, indicating that O_3 formation was generally VOC-limited in Wuhan. The effect of NHC on O_3 production was extremely limited according to its RIR, which was about two magnitudes lower than that of AHC. The RIR of CO was positive and extraordinarily high in Wuhan, indicating that CO was an important contributor to O_3, perhaps due to its extremely high concentration (mean = 1.6 ppmv). Conversely, the RIR of NO was generally negative, suggesting that NO suppressed the photochemical formation of O_3; that is, O_3 was titrated by NO. However, in July 2013, the RIR of NO was positive, implying that O_3 formation in this month was also partially NO_x-limited. The result was in line with the highest VOCs/NO_x ratio (1.3 ppbv/ppbv) with a relative abundance of VOCs and NO_x in July 2013, which was within the sampling period.

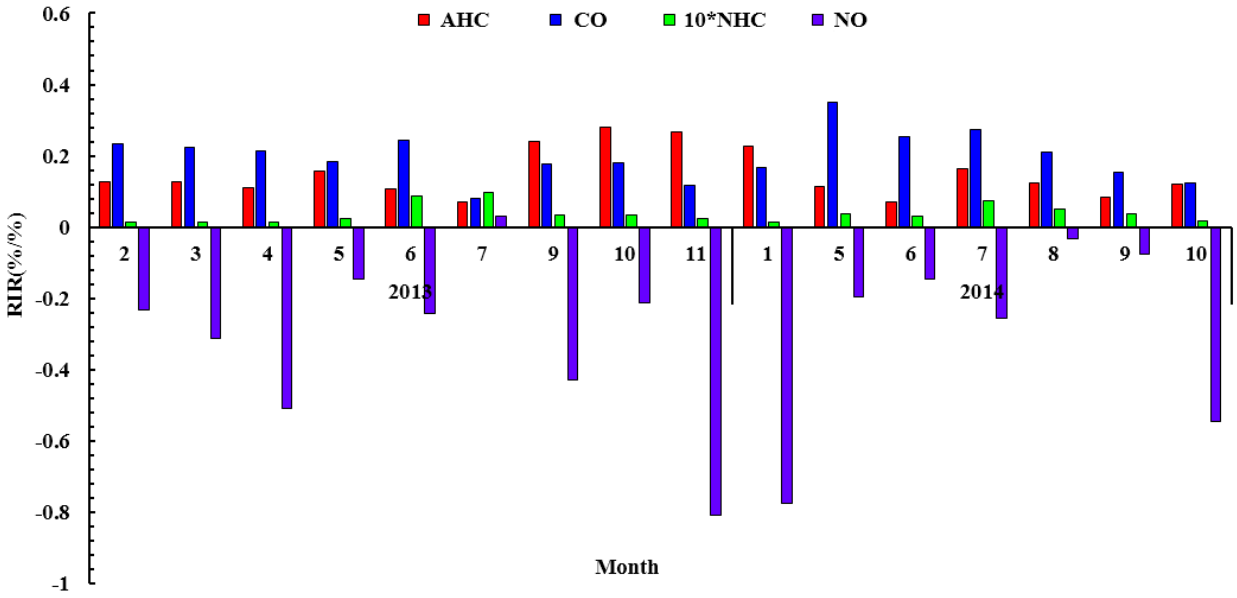

Figure 7 Monthly average RIR of AHC, CO, NHC, and NO. The RIR of NHC was amplified 10 times. The missed month was due to instrument maintenance.

To study the effect of individual VOC species on O_3 production, average RIR values of VOC species were calculated. Figure 8(a) shows the top VOCs with their RIR values. Alkenes (ethene, *trans*-2-butene, propene, and 1-butene) and aromatics (toluene and *m, p*-xylene) were the most reactive VOC species in Wuhan, consistent with the findings reported in the PRD region (Zhang et al., 2008; Ling and Guo, 2014). Regarding individual species, ethene and toluene had the highest RIR in Wuhan, while propene had the highest in Guangzhou (Zhang et al., 2008), and *m*-xylene and isoprene were the most reactive species in Hong Kong (Ling and Guo, 2014).

3.4.2 RIR-weighted concentration

It is well known that O_3 production is influenced by both the reactivity and concentration of VOCs. To enable further evaluation of the actual effect of VOC species on O_3 production, the calculated RIR-weighted concentration is given in Figure 8(b). Ethene and toluene were found to have the greatest effect on O_3 production in Wuhan, contributing 34.3% and 31.5% to the total RIR-weighted concentration, respectively. Cutting ethene and toluene would therefore be effective in controlling O_3 pollution in Wuhan. Table 5 presents the RIR-weighed concentrations of major VOCs for each source. The main contributors to O_3 production were found to be ethene, in vehicular exhausts, coal burning, and the petrochemical industry, and toluene, in coal burning

and solvent usage (in dry cleaning/degreasing and in coating/painting). Considerable contributions to O_3 production were made by C_4 alkanes (*n*/*i*-butanes), alkenes (*trans*-2-butene and 1-butene), and *m, p*-xylene when the source was LPG usage, in addition to ethene and toluene. This can inform VOC source emission control for the reduction of O_3 in Wuhan.

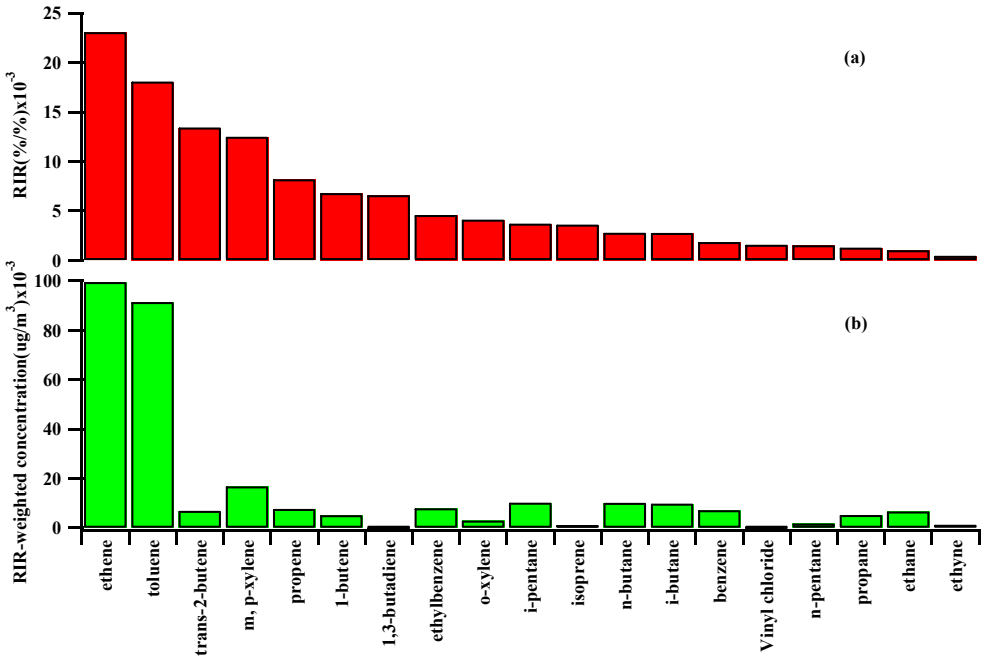

Figure 8 (a) Average RIR and (b) RIR-weighted concentration of individual VOC species

Table 5 RIR-weighted concentrations of VOCs in each source ($\mu g/m^3 \times 10^{-3}$)

	Vehicular exhausts	Coal burning	LPG usage	Petrochemical industry	Dry cleaning/ degreasing	Painting/ coating
Ethene	52.2	28.8	5.5	12.9		
i-Butane	0.3		7.3	1.9		0.1
n-Butane	0.2		7.7	2.1		0.2
trans-2-Butene	0.4		6.0	0.2	0.1	0.2
1-Butene	0.8		3.6	0.4		0.1
Toluene	6.2	44.0	9.8	0.9	10.8	19.6
m, p-Xylene		5.9	3.6		0.6	6.7

4. Conclusions

In this study, VOCs were continuously measured at an urban site in Wuhan from February 2013 to October 2014. Of the Chinese megacities, Wuhan has a relatively low level of TVOCs. Ethane, ethene, and toluene were the most abundant VOC species. The most significant contribution to both VOCs (27.8 ± 0.9%) and O_3 production (23.4 ± 1.3) was from vehicular exhausts. The contributions of LPG and solvent usage in coating/painting to O_3 production were higher than their contributions to VOCs. RIR calculation indicated that the photochemical O_3 formation in Wuhan was generally VOC-limited, and ethene and toluene had the highest effect on O_3 production. Additionally, the contribution of CO to O_3 production cannot be neglected, in view of its high RIR. Source apportionment of RIR-weighted concentrations of VOCs suggested that ethene in vehicular exhausts and coal burning, toluene in vehicular exhausts, coal burning, LPG usage, and solvent usage, and the C_4 alkanes in LPG usage were the main contributors to O_3 formation in Wuhan. This study is the first to provide empirical evidence that can contribute to the effective reduction of VOCs and O_3 in Wuhan.

Acknowledgements

This project was supported by the exchange project between Hong Kong and Mainland China Universities, the Research Grants Council of the Hong Kong Special Administrative Region (PolyU5154/13E and PolyU152052/14E), and the Hong Kong Polytechnic University Ph.D. scholarships (project #RTUP). This study is partly supported by the Public Policy Research Funding Scheme (2013.A6.012.13A) and the National Natural Science Foundation of China (No. 41405112).

References:

An, J.L., Zhu, B., Wang, H.L., Li, Y.Y., Lin, X., Yang, H., 2014. Characteristics and source apportionment of VOCs measured in an industrial area of Nanjing, Yangtze River Delta, China. Atmos. Environ. 97, 206-214.

Atkinson, R., 1990. Gas-phase tropospheric chemistry of organic compounds: a review. Atmos. Environ. 24, 1-41.

Barletta, B., Meinardi, S., Rowland, F.S., Chan, C.Y., Wang, X.M., Zou, S.C., Chan, L.Y., Blake, D.R., 2005. Volatile organic compounds in 43 Chinese cities. Atmos. Environ. 39, 5979-5990.

Barletta, B., Meinardi, S., Simpson, I.J., Khwaja, H.A., Blake, D.R., Rowland, F.S., 2002. Mixing ratios of volatile organic compounds (VOCs) in the atmosphere of Karachi, Pakistan. Atmos. Environ. 36, 3429-3443.

Cai, C.J., Geng, F.H., Tie, X.X., Yu, Q., An, J.L., 2010. Characteristics and source apportionment of VOCs measured in Shanghai, China. Atmos. Environ. 44, 5005-5014.

Camredon, M., Aumont, B., Lee-Taylor, J., Madronich, S., 2007. The SOA/VOC/NO_x system: an explicit model of secondary organic aerosol formation. Atmos. Chem. Phys. 7, 5599-5610.

Carter, W.L., Atkinson, R., 1989. Computer modeling study of incremental hydrocarbon reactivity. Environ. Sci. and Tech. 23, 864-880.

Cetin, E., Odabasi, M., Seyfioglu, R., 2003. Ambient volatile organic compound (VOC) concentrations around a petrochemical complex and a petroleum refinery. Sci. Total Environ. 312, 103-112.

Chan, C.K., Yao, X.H., 2008. Air pollution in mega cities in China. Atmos. Environ. 42, 1-42.

Chang, S.C., Lee, C.T., 2007. Evaluation of the trend of air quality in Taipei, Taiwan from 1994 to 2003. Environ. Mont. Assess. 127, 87-96.

Cheng, H.R., Guo, H., Saunders, S.M., Lam, S.H.M., Jiang, F., Wang, X.M., Wang, T.J., 2010. Assessing photochemical ozone formation in the Pearl River Delta using a photochemical trajectory model. Atmos. Environ. 44, 4199-4208.

Cheng, H.R., Saunders, S.M., Guo, H., Louie, P.K.K., Jiang, F., 2013. Photochemical trajectory modeling of ozone concentrations in Hong Kong. Environ. Pollut. 180, 101-110.

Ding, A.J., Wang, T., Thouret, V., Cammas, J.P., Nedelec P., 2008. Tropospheric ozone climatology over Beijing: analysis of aircraft data from the MOZAIC program. Atmos. Chem. Phys. 8, 1-13.

Dufour, G., Eremenko, M., Orphal, J., Flaud, J.M., 2010. IASI observations of seasonal and day-to-day variations of trospheric ozone over three highly populated areas of China: Beijing, Shanghai, and Hong Kong. Atmos. Chem. Phys. 10, 3787-3801.

Geng, F.H., Zhang, Q., Tie, X.X., Huang, M.Y., Ma, X.C., Deng, Z.Z., Yu, Q., Quan, J.N., Zhao, C.S., 2009. Aircraft measurements of O_3, NO_x, CO, VOCs, and SO_2 in the Yangtze River Delta region. Atmos. Environ. 43, 584-593.

Guo, H., Cheng, H.R., Ling, Z.H., Louie, P.K.K., Ayoko, G., 2011. Which emission sources are responsible for the volatile organic compounds in the atmosphere of Pearl River Delta? J. Hazard. Mater. 188, 116-124.

Guo, H., Ling, Z.H., Cheung, K., Jiang, F., Wang, D.W., Simpson, I.J., Barletta, B., Meinardi, S., Wang, T.J., Wang, X.M., Saunders, S.M., Blake, D.R., 2013. Characterization of photochemical pollution at different elevations in mountainous areas in Hong Kong. Atmos. Chem. Phys. 13, 3881-3898.

Guo, H., So, K.L., Simpson, I.J., Barletta, B., Meinardi, S., Blake, D.R., 2007. C_1-C_8 volatile organic compounds in the atmosphere of Hong Kong: Overview of atmospheric processing and source apportionment. Atmos. Environ. 41, 1456-1472.

Guo, H., Wang, T., Louie, P.K.K., 2004. Source apportionment of ambient non-methane hydrocarbons in Hong Kong: Application of a principal component analysis/absolute principal component scores (PCA/APCS) receptor model. Environ. Pollut. 129, 489-498.

Huang, B.B., Lei, C., Wei, C.H., Zeng, G.M., 2014. Chlorinated volatile organic compounds (Cl-VOCs) in Environment-sources, potential human health impacts, and current remediation technologies. Environ. Int. 71, 118-138.

Huang, C., Chen C.H., Li, L., Cheng, Z., Wang, H.L., Huang, H.Y., Streets, D.G., Wang, Y.J., Zhang, G.F., Chen Y.R., 2011. Emission inventory of anthropogenic air pollutants and VOC species in the Yangtze River Delta region, China. Atmos. Chem. Phys. 11, 4105-4120.

Huang, J.P., Fung, J.C.H., Lau, A.K.H., Qin, Y., 2005. Numerical simulation and process analysis of typhoon-related O_3 episodes in Hong Kong. J. Geophys. Res. 110, D05301, doi:10.1029/2004JD004914.

Jenkin, M.E., Hayman, G.D., 1999. Photochemical ozone creation potentials for oxygenated volatile organic compounds: sensitivity to variations in kinetic and mechanistic parameters. Atmos. Environ. 33, 1275-1293.

Kim, J.H., Lee, H.J., Lee S.H., 2006. The characteristics of tropospheric ozone seasonality observed from ozone soundings at Pohang, Korea. Environ. Monit. Assess. 118, 1-12.

Kwon, H.S., Lee, S.H., 2003. Phase Behavior of poly (ethylene-co-norbornene) in C_6 hydrocarbon solvents: effect of polymer concentration and solvent structure. Macromol. Res. 11, 231-235.

Lam, S.H.M., Saunders, S.M., Guo, H., Ling, Z.H., Jiang, F., Wang, X.M., Wang, T.J., 2013. Modelling VOC source impacts on high ozone episode days observed at a mountain summit in Hong Kong under the influence of mountain-valley breezes. Atmos. Environ. 81, 166-176.

Lash, L.H., Parker, J.C., 2001. Hepatic and renal toxicities associated with perchloroethylene. Pharmacol. Rev. 53, 177-208.

Li, X., Cai, C.J., Zhu, B., An, J.L., Li, Y.Y., Li, Y., 2014. Source apportionment of VOCs in a suburb of Nanjing, China, in autumn and winter. J. Atmos. Chem. 71, 175-193.

Ling, Z.H., Guo, H., 2014. Contribution of VOC sources to photochemical ozone formation and its control policy implication in Hong Kong. Environ Sci. Policy. 38, 180-191.

Ling, Z.H., Guo, H., Cheng, H.R., Yu, Y.F., 2011. Sources of ambient volatile organic compounds and their contributions to photochemical ozone formation at a site in the Pearl River Delta, southern China. Environ. Pollut. 159, 2310-2319.

Ling, Z.H., Guo, H., Lam, S.H.M., Saunders, S.M., Wang, T., 2014. Atmospheric photochemical reactivity and ozone production at two sites in Hong Kong: Application of a Master Chemical Mechanism-photochemical box model. J. Geophys. Res. Atmos. 119, 10,567-10,582, doi:10.1002/ 2014JD021794.

Liu, Y., Shao, M., Lu, S.H., Chang, C.C., Wang, J.L., Chen, G., 2008a. Volatile Organic Compound (VOC) measurements in the Pearl River Delta (PRD) region, China. Atmos. Chem. Phys. 8, 1531-1545.

Liu, Y., Shao, M., Lu, S.H., Chang, C.C., Wang, J.L., Fu, L.L., 2008b. Source apportionment of ambient volatile organic compounds in the Pearl River Delta, China: Part II. Atmos. Environ. 42, 6261-6274.

Liu, Y., Shao, M., Zhang J., Fu L.L., Lu, S.H., 2005. Distributions and source apportionment of ambient volatile organic compounds in Beijing city, China. J. Environ. Sci. Heal. 40, 1843-1860.

Lyu, X.P., Wang, Z.W., Cheng, H.R., Zhang, F., Zhang, G., Wang, X.M., Ling, Z.H., Wang, N., 2015. Chemical characteristics of submicron particulates ($PM_{1.0}$) in Wuhan, central China. Atmos. Res. 161-162, 169-178.

McCarthy, M.C., Aklilu, Y.A., Brown, S.G., Lyder, D.A., 2013. Source apportionment of volatile organic compounds measured in Edmonton, Alberta. Atmos. Environ. 80, 504-516.

Morrow, N.L., 1990. The industrial production and use of 1,3-butadiene. Environ. Health Persp. 86, 7-8.

Na, K., Kim, Y.P., Moon, K.C., Moon, I., Fung, K., 2001. Concentrations of volatile organic compounds in an industrial area of Korea. Atmos. Environ. 35, 2747-2756.

Ou, J.M., Guo, H., Zheng, J.Y., Cheung, K., Louie, P.K.K., Ling, Z.H., Wang, D.W., 2015. Concentrations and sources of non-methane hydrocarbons (NMHCs) from 2005 to 2013 in Hong Kong: A multi-year real-time data analysis. Atmos. Environ. 103, 196-206.

Paatero, P., Tapper, U., 1994. Positive matrix factorization: A non-negative factor model with optimal utilization of error estimates of data values. Environmetrics, 5, 111-126.

Paatero, P., 1997. Least squares formulation of robust non-negative factor analysis. Chemom. Intell. Lab. Sys. 37, 23-35.

Saunders, S.M., Jenjin, M.E., Derwent, R.G., Pilling, M.J., 2003. Protocol for the development of the Master Chemical Mechanism, MCM v3 (Part A): tropospheric degradation of non-aromatic volatile organic compounds. Atmos. Chem. Phys. 3, 161-180.

Sharkey, T.D., Singsaas, E.L., Vanderveer, P.J., Geron, C., 1996. Field measurements of isoprene emission from trees in response to temperature and light. Tree Phys. 16, 649-654.

Song, Y., Dai, W., Shao, M., Liu, Y., Lu, S.H., Kuster, W., Goldan, P., 2008. Comparison of receptor models for source apportionment of volatile organic compounds in Beijing, China. Environ. Pollut. 156, 174-183.

Song, Y., Shao, M., Liu, Y., Lu, S.H., Kuster, W., Goldan, P., Xie, S.D., 2007. Source apportionment of ambient volatile organic compounds in Beijing. Environ. Sci. Technol. 41, 4348-4353.

Tsigaridis, K., Lathiere, J., Kanakidou, M., Hauglustaine, D. A., 2005. Naturally driven variability in the global secondary organic aerosol over a decade. Atmos. Chem. Phys. 5, 1891-1904.

Wang, M., Shao, M., Lu, S.H., Yang, Y.D., Chen, W.T., 2013. Evidence of coal combustion contribution to ambient VOCs during winter in Beijing. Chinese Chem. Lett. 24, 829-832.

Wang, T., Wei, X.L., Ding, A.J., Poon, C.N., Lam, K.S., Li, Y.S., Chan, L.Y., Anson, M., 2009. Increasing surface ozone concentrations in the background atmosphere of Southern China. Atmos. Chem. Phys. 9, 6217-6227.

Warneck, P., 2000. Chemistry of the Natural Atmosphere. Academic Press, San Diego, CA, pp. 266-267.

Wei, W., Cheng, S.Y., Li, G.H., Wang, G., Wang, H.Y., 2014. Characteristics of volatile organic compounds (VOCs) emitted from a petroleum refinery in Beijing, China. Atmos. Environ. 89, 358-366.

Xue, L.K., Wang, T., Gao, J., Ding, A.J., Zhou, X.H., Blake, D.R., Wang, X.F., Saunders, S.M., Fan, S.J., Zuo, H.C., Zhang, Q.Z., Wang, W.X., 2014. Ground-level ozone in four Chinese cities: precursors, regional transport and heterogeneous processes. Atmos. Chem. Phys. 14, 13175-13188.

Yao, Z.L., Shen, X.B., Ye, Y., Cao, X.Y., Jiang, X., Zhang, Y.Z., He, K.B., 2015. On-road emission characteristics of VOCs from diesel trucks in Beijing, China. Atmos. Environ. 103, 87-93.

Zhang, Y.H., Su, H., Zhong, L.J., Cheng, Y.F., Zeng, L.M., Wang, X.S., Xiang, Y.R., Wang, J.L., Gao, D.F., Shao, M., Fan, S.J., Liu, S.C., 2008. Regional ozone pollution and observation-based approach for analyzing ozone-precursor relationship during the PRIDE-PRD2004 campaign. Atmos. Environ. 42, 6203-6218.